MacAreno LM, Angulo C, López D, Agirrebeitia J. *Analysis and characterization of the behaviour of a variable geometry structure*. **Proceedings of the Institution of Mechanical Engineers, Part C: Journal of Mechanical Engineering Science**. 2007;221(11):1427-1434. https://doi.org/10.1243/09544062JMES612.

Analysis and characterization of the behaviour of a variable geometry structure.

L M Macareno, C Angulo, D López, and **J Agirrebeitia**
Department of Mechanical Engineering, University of the Basque Country UPV/EHU, Escuela Técnica Superior de Ingeniería (ETSI), Bilbao, Vizcaya, Spain

Abstract: The study about a variable geometry truss is presented. The first step is a kinematic design and later an analysis using the MSC/Adams code. Then, the finite-element method with the MSC/Nastran code was used to develop a variable mathematical model to characterize its mechanical behaviour. An explanation is given of the solution selected to analyze the most complex joints. A series of measurements were carried out using different experimental techniques. The aim of photogrammetry tests is to study clearance effect in the joints. On the other hand, measurements of the stiffness were carried out to introduce these data in the finite-element model and thus characterize the accurate position of the structure.

Keywords: variable geometry truss, finite element, joints, clearances, measurement, behavior

1 INTRODUCTION

At the beginning of the 1980s study began on the so called variable geometry structures mainly for space use [1, 2]. Their capacity to adapt to different mechanical solicitations varying their geometry [3, 4] and high stiffness to weight ratio make them highly appropriate for this purpose. Nowadays, the study of these structures is focused in tensegrity structures [5], deployable structures [6], and adaptive structures [7], where new materials and components are being tested. Their most immediate application is as manipulators or antenna masts [8]. The most common shape of these structures is the spatial truss, comprising various bays or modules, where the basic unit is repeated. Several studies exist showing the characteristics of the different geometrical shapes, which can be used as the basic unit. In this case, the octahedron has been chosen (Fig. 1), with the actuators on the horizontal planes [9–11]. For the current study, a five-bay prototype was built with four actuator planes, as shown in Fig. 2. There are three actuator bars on each plane, which may vary in length, forming an equilateral triangle in their initial position. These bars are connected by special nodes with various types of kinematic pairs: two rotational and four spherical. The rotational pairs join the actuators to the central section of the node and the spherical pairs connect the other bars, two at the top and two at the bottom. These bars join the different planes to each other. The five-bay structure has 12 degrees-of-freedom (DOFs). A kinematic model was developed using the MSC/Adams code, with which the structure kinematic variables can be known at any given moment. In addition, a Patran Command Language (PCL) program was used to create a finite-element model from an IGES file obtained through MSC/Adams, and subsequently studied using MSC/Patran code. This program enables the creation of as many finite-element models as desired for each structure position. Thus, the effect of the different structure elements on final positions may be studied in greater depth. Adjustment of these models was carried out via extensiometry and photogrammetry testing.

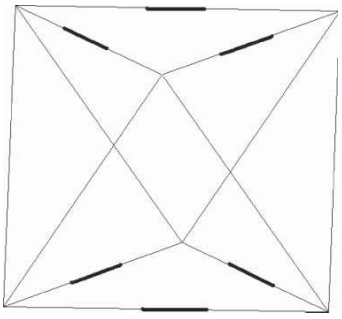

Fig. 1 Basic unit. Octahedron

2 MATHEMATICAL MODELS

The variable geometry truss (VGT) prototype is based on theoretical geometry using an octahedron as the basic unit. This geometry repeats itself throughout the five bays, obtaining a three-dimensional truss comprising 48 bars. The three bars on the base and the three at the top of the triangle have a constant length and are called ‘battens’. The 12 bars on the other parallel planes are called ‘actuators’ and may vary in length [12]. The remaining 30 bars which communicate the different planes are called ‘longerons’ and whose length is constant. All the structure bars are joined together at the nodes. In fact, it is impossible for the bars to be connected to a single point; therefore, a node as close as possible to the ideal has been designed. Six bars are connected to this node: two actuators and four longerons, as shown in Fig. 3.

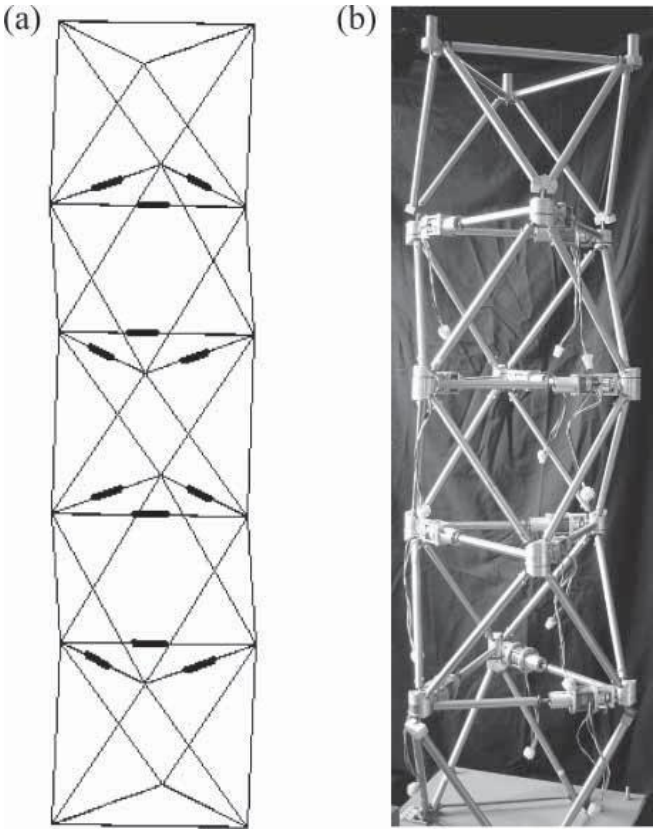

Fig. 2 (a) Five-bay geometrical diagram and (b) real prototype

The actuators are connected to the node via two rotational pairs and the longerons with spherical bearings. These nodes are repeated on all the intermediate bays. Nevertheless, three spherical bearings are sufficient on the upper and lower end nodes. This is because the bars joining the base plane to the one above have no relative movement between them, are two by two, and thus joined at the node by a single spherical bearing. The same situation occurs symmetrically in the bars joining the upper plane end to the one immediately below. These bars are likewise joined to the end planes with spherical bearings. The actuator bars consist of a brake, an electric stepper motor, a coupling, and a precision ball screw. Figure 4 shows a longitudinal view where these elements can be observed. At the ends there are two rings forming the rotational pairs on the nodes. The kinematic model can be carried out with all these data on MSC/Adams. Two models were developed; the most complex based on the part manufacturing drawings representing all the elements, including the nodes in detail. This model was used to perform several simulations of interest, visualizing the rotation angles on the bearings and possible contacts which might occur. Figure 5 shows the realistic kinematic model of the prototype. The second model was more straightforward, including only the elemental geometry; and is known as the structure ‘skeleton’. This model was used as a base for construction of the final finite-element model in a subsequent phase. Execution sequence is as follows: first, using the MSC/Adams code a specific position is analyzed and then geometry is exported to the MSC/Patran code via IGES file. Immediately afterwards, the

macro program in PCL is executed obtaining a complete finite-element model, where different load cases can be simulated. Program is based on the imported geometry reference points. The most complex elements, i.e. the nodes, were previously modelled in other files. These submodels are inserted in the final model. Relative reference systems are created and subsequently aligned to situate all the elements in their correct orientation. Element properties, such as materials or section may be easily modified in the program.

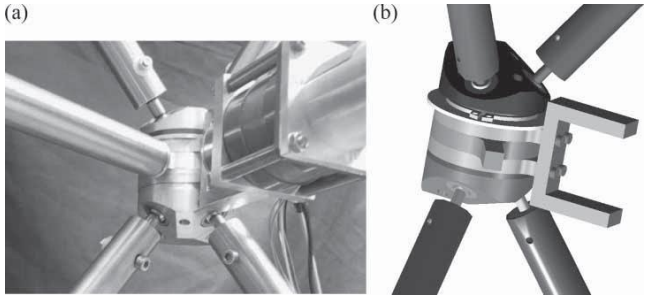

Fig. 3 Detail of (a) real prototype node and (b) model node

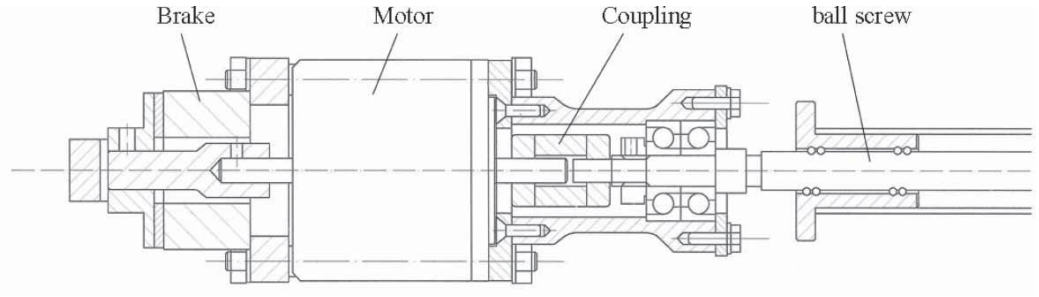

Fig. 4 Longitudinal view of the actuator bar

This development enables accurate study of all the structure positions of interest. Development diagram is shown in Fig. 6. In finite-element design, modelling of the different parts comprising the prototype must be defined [13]. Basically, three element types were used: three-dimensional beams, three-dimensional solids (tetrahedron and hexahedron) and springs (both axial and torsion). For truss configuration of the structure, it is deduced that the efforts supported are basically axial, in most cases, traction on actuators and compression on longerons. Among all the elements comprising the structure, the coupling presents greater flexibility, suffering deformations of a magnitude considerably higher than the other components. Its longitudinal stiffness was modelled using a spring element. Stiffness in the transversal direction has a small influence on the global structure behaviour and was also modelled using spring elements. The other actuator elements were modelled via beam elements of different lengths, sections, and materials. The longerons were correctly modelled using beam elements, with the tube section. Nodes were represented via three-dimensional elements to correctly define their shape. As said before, these nodes join six bars, four longerons, and two actuators. These are joined to the nodes via multi-point constraints. Thus a series of equations relating different DOFs is defined on MSC/Patran. This method must be used since a beam element (six DOFs on each node) is to be joined to a three-dimensional element (three DOFs per node) so it functions like a clamp. There are different methods which provide values with minor distortion in relation to the stress distribution on either side of the connection [14, 15]. However, in this case, it was not of particular interest because the axial stress is the predominant. Therefore, it was decided to use a linear equation relating the node rotational DOFs of the beam element to the displacements of the three-dimensional elements next to this node.

On the other hand, the nodes and the longerons are joined by as many spherical bearings. These bearings consist of a fixed body joined to the node and a spherical mobile part. Modelling in detail of this element offers no improvement for the model, so it was decided to use spring elements to represent the stiffness of the bearing body in the three directions. The spherical pairs include the clearance effect [16, 17] bearing in mind the experimental results carried out previously.

To consider this effect a spring–damper model commonly used in the study of clearances in multi-body systems was employed. The bearing rotation is simulated considering pinned DOFs on the transversal axes (Ry , Rz). Even though the bearing can also rotate on its longitudinal axis, this condition was not included in the model since it was redundant and had no influence on the global structure displacement. The model is clamped to its base and the loads are applied on the vertices of the upper triangle. Details of the finite-element model are shown in Figs 7 and 8.

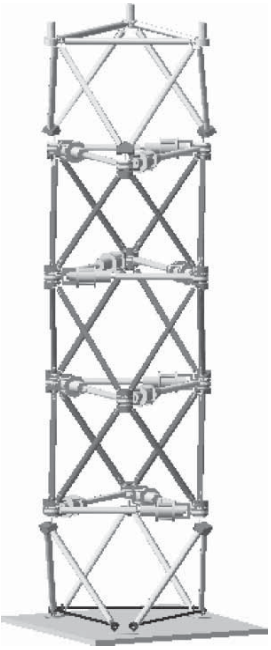

Fig. 5 Realistic kinematic model on MSC/Adams

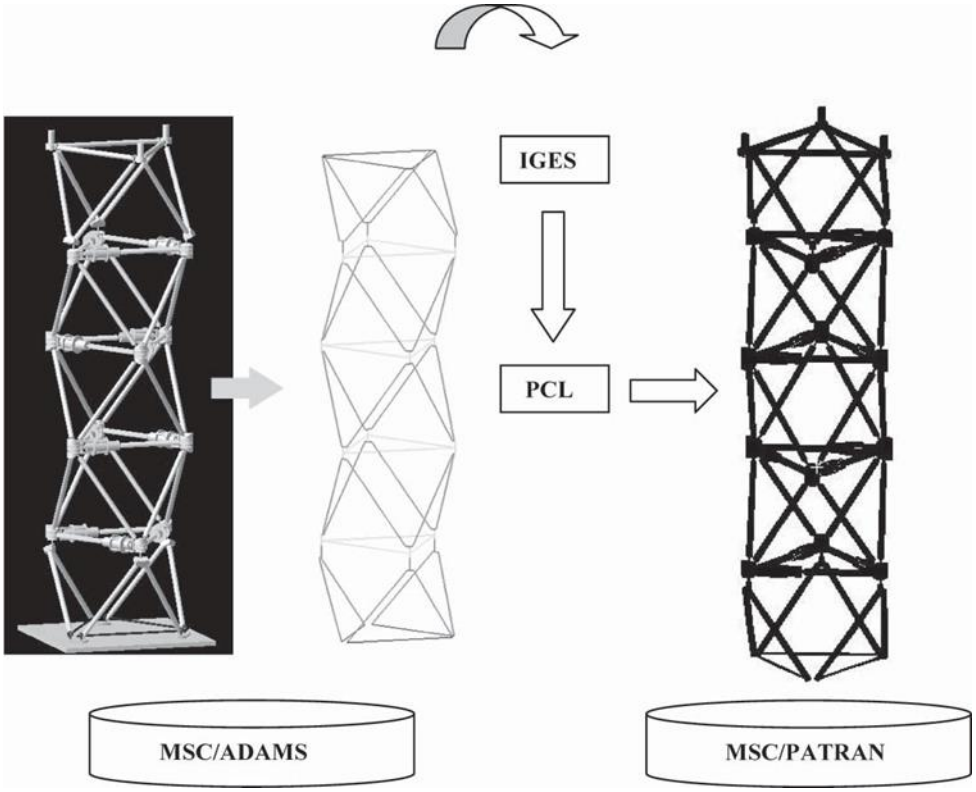

Fig. 6 Development diagram of the finite-element model

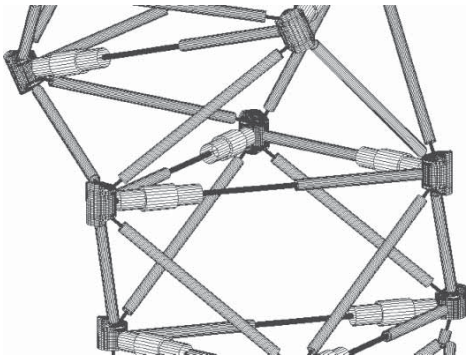

Fig. 7 Actuator plane

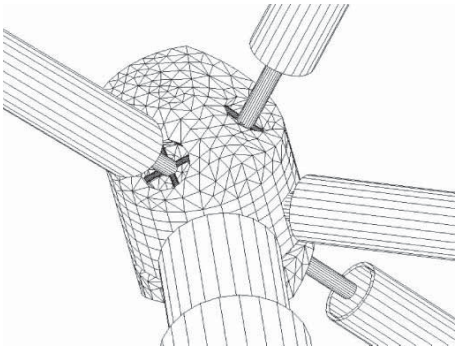

Fig. 8 Intermediate node

3 TESTING

Once the finite-element model was developed, two different kinds of tests were performed to evaluate some of the system variables. Thus, the VGT prototype real behaviour can be characterized more accurately:

The aim of the first test type was to determine the repeatability of the structure, i.e. the capacity to return to its original position after performing a series of movements. Tests were performed in the case of the structure vertical displacement. There are several optical techniques that can be used for displacements measurements [18]. In this case photogrammetry techniques without contact were used to measure the repeatability. These techniques are appropriate when the point to measure is not easily accessible or when the techniques themselves can influence on the results. The equipment consists on a digital camera Nikon D100 with a six mega pixels image sensor, an objective Nikkor of 300 mm and a teleconverter of 1.4 (resulting in a focal length of 420 mm). The camera is assembled on a very rigid tripod and a control program to shoot and register the pictures is used, so any small movement is aborted. This software is the Nikon Capture Camera Control. Figure 9 shows the camera and the tripod. A closely orthographic projection is obtained with the focal length and the distance between the camera and the structure, 5 m, so perspective distortion is not taken into account. Thus photographs can be processed directly, without data preprocessing. A grid has been developed as a reference for the measurements. This grid has been calibrated using a microscope model Mitutoyo TM with micrometer heads on x and y-directions. The grid, situated on a vertex of the upper triangle, is shown in Fig. 10. A computer is connected to the camera via USB connection and to the drivers via RS232 series connection. The drivers move the electric motors of the actuators following the given instructions. These instructions are introduced by the user through the specific software developed for these drivers. The basic functions are the definition of the displacement, velocity, and acceleration of the electric motor.

Fig. 9 Camera and tripod

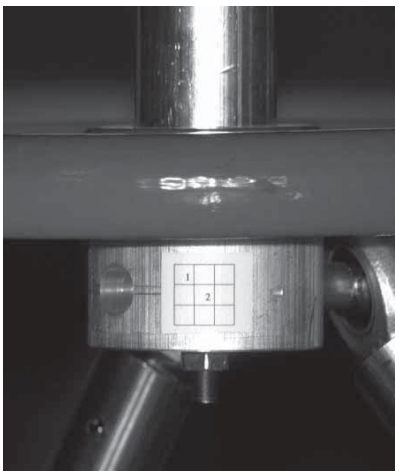

Fig. 10 Calibrated grid

Tests were performed with the structure in vertical position, moving all the actuators on the same plane at the same time, thereby achieving a rectilinear movement on the vertical axis. Measurements were taken for several load cases and actuator displacements in the initial and return positions. The coordinates of two grid points are obtained from each picture, so any possible error on data acquisition can be easily detected. Results were also checked with the use of dial gauges. These results agree with those previously obtained for the three-bay structure [19]. It can be assumed that positioning errors come from clearances in the spherical bearings. Results are shown in Fig. 11. The relative error is calculated for each case as the quotient of the difference between the initial and return positions and the vertical displacement. The second test type was performed to measure the stiffness of the flexible couplings which form part of the actuator bars. A traction-testing machine was used, adapting it to the coupling case. Figure 12 shows the machine in its initial position, before the coupling had suffered any deformation. The stiffness is obtained as the slope of the curve force-deformation as shown in Fig. 13, corresponding to a value of 2.5 104 N/m. This curve is linear in the usual range of load cases for the current study. In the mathematical model, it has been included only the linear model, not considering the plastic behaviour.

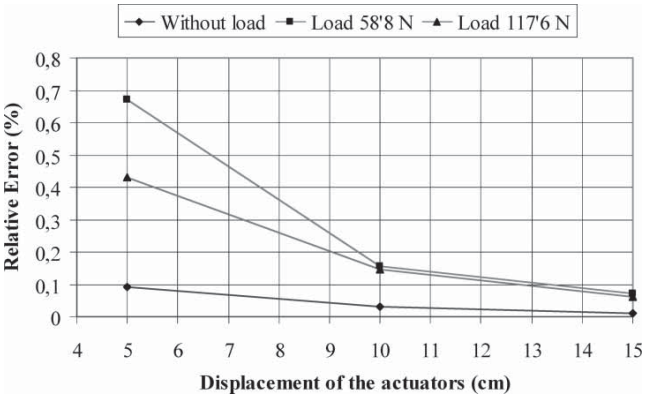

Fig. 11 Relative error in vertical displacement

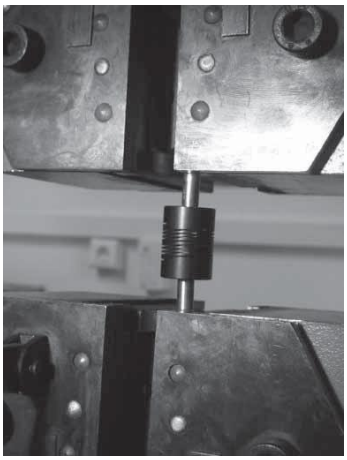

Fig. 12 Traction-testing machine

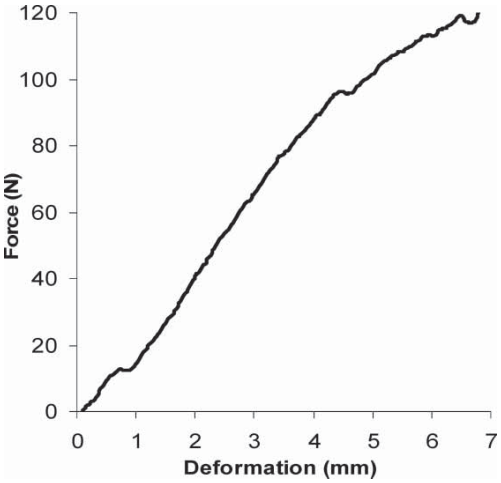

Fig. 13 Curve force-deformation of the coupling

4 RESULTS

The properties of the couplings and the bearings have been defined from data obtained in the tests. Couplings are modelled with spring elements whose stiffness has been defined previously. Spherical bearings are modelled by a stiffness representing the effect of the clearances. It is considered that all the bearings have the same stiffness. This value is obtained from the absolute displacements and forces of the photogrammetry tests. With this method an approximation of the real behaviour of the bearings is supposed, but it is useful in a qualitative point of view. The other elements of the model are defined through their physical properties. Longerons are steel tubes. The rods that join the tubes with the bearings are made of brass. The elements forming the nodes are of aluminum. The elements of the

actuator bars have their own specification sheets, so the characteristics can be obtained from them. By way of verification, an analytical calculation was carried out on the forces acting on all the structure bars, using a mathematical structure made up of ideal octahedrons forming a three-dimensional truss. Calculations were reduced to the range of positions on the vertical axis, which was the case used for testing. The obtained results are very close to those shown by the finite-element model. This model allows the differentiation among the deformation components because of the couplings, the bearings, and the other elements. In order to obtain a movement of the structure in the vertical axis, the three actuators of the same horizontal plane must vary their length identically. The initial position of the structure is considered the reference of the actuator displacement. In this case the value of the displacement is zero. The study consists on the five positions obtained from the following displacements of the actuators: 0, 50, 100, 150, and 200 mm, moving simultaneously. Load cases vary from 10 to 100 N, with increments of 10 N. The total number is five positions and ten load cases in each. The loads are applied on each of the vertices of the upper triangle, so the maximum load over the entire structure is 300 N. Figure 14 shows the different positions of the structure and the reference point where measurements are taken. Table 1 shows the results for the ten load cases in the initial position. The displacement column shows the total vertical displacement of the reference point. This value has been obtained from MSC/Nastran.

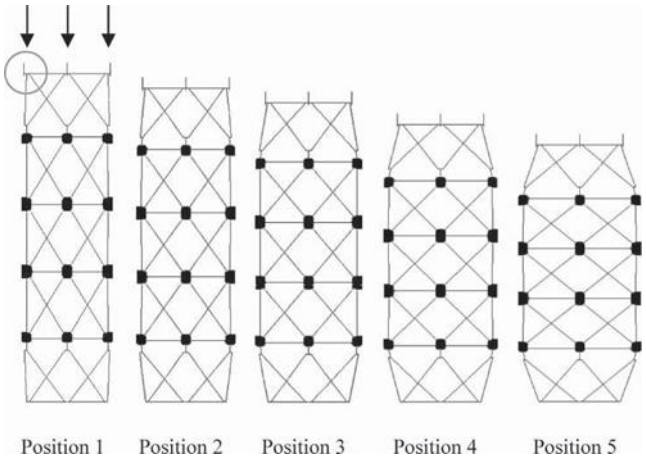

Fig. 14 Positions of the structure

Load (N)	Displacement (mm)	Coupling	%	Bearing	%	Others	%
10	1.79	1.51	84.47	0.20	10.97	0.08	4.56
20	2.10	1.78	84.74	0.23	11.00	0.09	4.26
30	2.42	2.05	84.60	0.27	10.98	0.11	4.43
40	2.73	2.32	84.80	0.30	11.00	0.11	4.20
50	3.04	2.58	84.97	0.34	11.02	0.12	4.01
60	3.36	2.85	84.85	0.37	11.00	0.14	4.14
70	3.67	3.12	84.99	0.40	11.02	0.15	3.99
80	3.99	3.39	84.90	0.44	11.00	0.16	4.09
90	4.30	3.66	85.03	0.47	11.02	0.17	3.96
100	4.62	3.92	84.95	0.51	11.00	0.19	4.04
		Mean	84.83	Mean	11.00	Mean	4.17

Table 1 Results for the ten load cases in the initial position

The coupling and bearing columns show the vertical components of the displacements because of each of these elements. Finally, the others column is the difference with the total. This last value is attributed to all the other deformable elements of the structure. The value of the percentages in relation to the total is included to the right of each column. It must be noticed that the values shown in the table are actually the components in the vertical direction because of each component. For example, couplings are part of the actuator bars and their deformation occurs in the longitudinal direction of those. This deformation implies a length variation of the actuators, which leads to a vertical movement of the structure. This last value is the one that appears on the table. The case of the bearing is something similar. The axes of the rods that joint them to the bars are in oblique planes. The table shows the components in the vertical direction. It can be noticed that the deformation because of the couplings means the main part of the total, in the order of 85 per cent. The bearings mean an 11 per cent and the rest of elementsa4 per cent. The deformation attribute to

the 'Others' term comes from bending and length variations of the bars of the structure. These percentages vary according to each position of the structure. Figure 15 shows the variation of the percentage of deformation because of the couplings. The percentage of deformation because of the bearings does not vary in the case of the displacement of the structure in the vertical direction. The increment of percentage goes to the other elements. The bars lean when the displacements of the actuators divided into three components: couplings, bearings, and other elements. The most important component of the deformation is due to the couplings, more than 80 per cent. This percentage varies for each position but it is always the greatest. With these refined models it is possible to accurately study the behaviour of the variable geometry truss, taking into account all the significant variables are greater. This increases the value of the forces and so the bending of the bars. Even so, there is not a great increment. It can be noticed that the best way to reduce the deformation is to act mainly on the axial stiffness of the couplings. The deformation in the vertical direction can be reduced up to 80 per cent increasing this value.

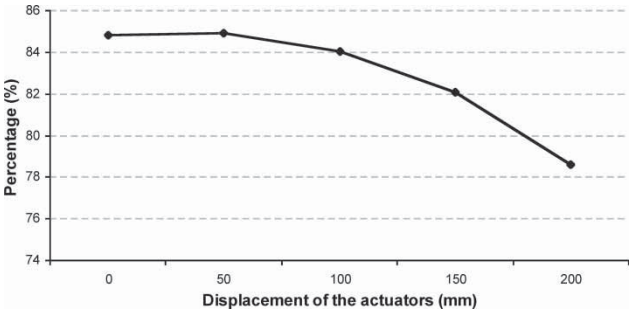

Fig. 15 Variation of the percentage of deformation because of the coupling

5 CONCLUSIONS

The current paper presents a study carried out with the aim to characterize the real behaviour of a variable geometry structure prototype. For this objective several mathematical models were created. Firstly, a kinematic one, which solves the positioning problem and subsequently a finite-element one for the strength study. On being a variable geometry structure, several models are required, whereby a procedure was developed which automatically creates a finite element model for the position of interest in each case. These models were correlated with the data obtained from the experimentation on this prototype. The techniques used for this study are the photogrammetry and traction tests.

The behaviour of the displacement of the structure is studied. The deformation in the vertical direction is divided into three components: couplings, bearings, and other elements. The most important component of the deformation is due to the couplings, more than 80 per cent. This percentage varies for each position but it is always the greatest. With these refined models it is possible to accurately study the behaviour of the variable geometry truss, taking into account all the significant variables.

ACKNOWLEDGEMENTS

The authors wish to acknowledge the financial support received from the Ministry of Education and Science of Spain, through the subsidy of research project DPI2005-05417.

REFERENCES

1 **Miura, K.** and **Furuya, H.** Adaptive structure concept for future space applications. *AIAA J.*, 1988, **26**(8), 995–1002.

2 **Haftka, R. T.** and **Adelman, H. M.** Selection of actuator locations for static shape control of large space structures by heuristic integer programming. *Comput. Struct.*, 1985, **20**, 575–582.

3 **Miki, M.** and **Koita, T.** Parallel computing for analysis of variable geometry trusses. *AIAA J.*, 1996, **34**(7), 1468–1473.

4 **Agirrebeitia, J., Avilés, R., de Bustos, I. F.,** and **Ajuria, G.** A method for the study of position in highly redundant multibody systems in environments with obstacles. *IEEE Trans. Robot. Autom.*, 2002, **18**(2), 257–262.

5 **Zhang, J. Y.** and **Ohsaki, M.** Stability conditions for tensegrity structures. *Int. J. Solids Struct.*, 2007, **44** (11–12), 3875–3886.

6 **Gruber, P., Häuplik, S., Imhof, B., Özdemir, K., Waclavicek, R.,** and **Perino, M. A.** Deployable structures for a human lunar base. *Acta Astronaut.*, 2007, **61**(1–6), 484–495.

7 **Benjeddou, A., Topping, B. H. V.,** and **Mota Soares, C. A.** Composite adaptive structures: modelling and simulation. *Comput. Struct.*, 2006, **84**(22–23), 1381–1383. **Chen, G.-S.** and **Wada, B.-K.** Adaptive truss manipulator space crane concept. *J. Spacecr. Rockets*, 1993, **30**(1), 111–115.

8 **Williams II, R. L.** and **Hexter, R. E.** Maximizing kinematic motion of a 3-dof VGT module. *J. Mech. Des.*, 1998, **120**(2), 333–336.

9 **Chen, W.-J., Luo, Y.-Z., Fu, G.-Y., Gong, J.-H.,** and **Dong, S.-L.** A study on space masts based on octahedral truss family. *Int. J. Space Struct.*, 2001, **16**(1), 75–82.

10 **Xu, L. J., Tian, G. Y., Duan,Y.,** and **Yang, S. X.** Inverse kinematic analysis for triple-octahedron variable-geometry truss manipulators. *Proc. Instn Mech. Engrs, Part C: J. Mechanical Engineering Science*, 2001, **215**(C2), 247–251.

11 **Dhingra, A. K.** and **Lee, B. H.** Optimal placement of actuators in actively controlled structures. *Eng. Optim.*, 1994, **23**, 99–118.

12 **Ramachandran, S., Nagarajan, T.,** and **Prasad, N. S.** A finite element approach to the design and dynamic analysis of platform type robot manipulators. *Finite Elem. Anal. Des.*, 1992, **10**, 335–350.

13 **Law, S. S., Chan, T. H. T.,** and **Wu, D.** Super-element with semi-rigid joints in model updating. *J. Sound Vibr.*, 2001, **239**(1), 19–39.

14 **Monaghan, D. J., Doherty, I. W., McCourt, D.,** and **Armstrong, C. G.** Coupling 1D beams to 3D bodies. In Proceedings of 7th International Meshing Roundtable, Sandia National Laboratories, Dearborn, Michigan, 1998, pp. 1–8.

15 **Ting, K., Zhu, J.,** and **Watkins, D.** The effects of joint clearance on position and orientation deviation of linkages and manipulators. *Mech. Mach. Theory*, 2000, **35**(3), 391–401.

16 **Zhu, J.** and **Ting, K.** Uncertainty analysis of planar and spatial robots with joint clearances. *Mech. Mach. Theory*, 2000, **35**(9), 1239–1256.

17 **Gonzalez, R., Cibrian, R., Pino, A., Soler, J.,** and **González, Y.** Displacement measurement in structural elements by optical techniques. *Opt. Lasers Eng.*, 2000, **34**, 75–85.

18 **Angulo, C., Macareno, L. M.,** and **López, D.** Analysis of the effect of clearances in the kinematics of adaptive structures. *IASME Trans.*, 2004, **1**(1), 36–42.